Title
UNIFORM SEMICLASSICAL ORBITAL CALCULATIONS OF HEAVY ION COULOMB EXCITATION

Authors
Massmann, Herbert
Rasmussen, John O.

Publication Date
1974-11-01

Submitted to Nuclear Physics B

LBL-3440
Preprint c.2

UNIFORM SEMICLASSICAL ORBITAL CALCULATIONS OF HEAVY ION COULOMB EXCITATION

Herbert Massmann and John O. Rasmussen

November 8, 1974

Prepared for the U. S. Atomic Energy Commission
under Contract W-7405-ENG-48

DISCLAIMER

Uniform Semiclassical Orbital Calculations of Heavy Ion Coulomb Excitation*.

Herbert Massmann** and John O. Rasmussen

Lawrence Berkeley Laboratory, U. of Calif.; Berkeley, Calif.

November 8, 1974

Abstract

A new semiclassical approach, which can be derived from Feynman's path integral formulation of quantum mechanics, is applied to multiple Coulomb excitation for backward scattering angles. The basic features of this method are that the dynamic of the problem is treated completely classically (that is, one solves classical equations of motion) but the quantum mechanical superposition principle is retained by evaluating a phase along the classical trajectory and adding probability amplitudes for indistinguishable processes rather than probabilities themselves. One finds even a quantitative agreement with the conventional De Boer - Winther code. The limit of sudden collision ($\xi = 0$) for $\eta \to \infty$ (η = Sommerfeld parameter) is evaluated analytically and is in very good agreement with results published for this case.

Contents

I. Introduction

With the recent availability of heavy ion beams at nuclear research energies, a new interest has arisen for semi-classical theoretical methods to explain the experimental results. For heavy ion scattering, coupled-channels quantum-mechanical calculations are beyond the capability of modern computers.

In this paper we wish to report on our exploration of uniform semiclassical approximation (USCA) orbital methods of the type developed and applied in recent years to molecular scattering and reaction problems [1-3]. In this method one uses the classical equations of motion to generate the semi-classical approximation to the time-independent quantum mechanical S matrix.

In the usual semiclassical approximation methods one treats the motion of the projectile classically, i.e. the radius vector $\vec{r}$ of the relative motion is assumed to be a well-defined function of time $\vec{r}(t)$. The interaction between the target and the projectile is treated quantum-mechanically, i.e. by solving the time-dependent Schrödinger-equation for an initial condition corresponding to the target nucleus in its ground state and numerically integrating the coupled-differential equations until a later time, when the interaction becomes negligible. A problem arising in this type of calculation is accounting for the effect the interaction has on the orbit of the projectile, which during the collision transfers energy, angular momentum or mass to the target. Some effort in solving this problem has recently been made for the case of

Coulomb Excitation [4]. In the USCA method however, this problem does not exist since one treats the dynamics of the system classically and solves this exactly. In the process of extracting the S matrix elements (or the excitation probabilities) however, one retains the quantum-mechanical superposition principle.

Section II presents the general equations of the USCA method. In this paper we will illustrate the USCA method for backward scattering ($\ell_{in}=0$) from an even-even deformed target, at energies below the Coulomb barrier. The equations of motion and the excitation probabilities for this example are written down in Section III. In Section IV the results of the numerical calculations are presented and discussed.

II Theory

The theoretical basis of the USCA orbital method has been given in great detail by Miller [1),3)] and in its application to nuclear physics in refs. 6,8), therefore we will give here only the results, referring to those papers for details.

Let r and p_r be the radial translational coordinate and momentum, and q and n the action angle variables describing classically a given "internal" degree of freedom of the system. The action variable n is the classical counterpart of the quantum number for this degree of freedom. The S matrix describing the transition between the "quantum" states n_1, n_2 is then given by:

$$S_{n_1 n_2} = \sum \frac{e^{i\Phi(n_1,n_2)}}{\sqrt{\frac{2\pi i}{\left(\frac{\partial^2 \Phi(n_1,n_2)}{\partial n_1 \partial n_2}\right)}}} \qquad (1)$$

where the phase Φ is given by:

$$\Phi(n_1,n_2) = -\frac{1}{\hbar}\int_{t_1\to-\infty}^{t_2\to+\infty} (r\dot{p}_r + q\dot{n})\, dt \qquad (2)$$

The sum in equation (1) goes over all possible classical paths that conserve energy and are such that $n(t_1)=n_1$ and $n(t_2)=n_2$. To find the paths, one solves the classical equations of motion for all possible initial conditions consistent with the restrictions mentioned above. Then one selects those values of q for which $n(t_2)=n_2$. The phase along this path is called $\Phi(n_1,n_2)$.

The equations (1) and (2) are usually derived from Feynman's path integral formulation of quantum mechanics. The semiclassical limit of matrix elements of quantum mechanical operators is found by invoking the stationary phase method to evaluate integrals. In the limit $\hbar \to 0$ the equations (1) and (2) become exact. Finally, we would like to mention that the periodicity of the angle variable q has as a consequence that $\Delta n = |n_2 - n_1|$ has to be an integer.

III Application to Coulomb Excitation

We will consider here only the case of backward scattering from an even-even deformed target at energies below the Coulomb barrier. By far the most important effect will then be Coulomb excitation. This is not of pure academic interest since in Coulomb excitation experiments one usually measures at backward scattering angles, since at those angles the excitation probability of high spin states is highest (as long as the center of mass energy is below the Coulomb barrier). In Table I, one can compare results, computed with the De Boer - Winther[5] semiclassical code for multiple Coulomb excitation, for the excitation probabilities at two different angles $\theta_{cm}=180^\circ$ and $\theta_{cm}=165$ for ^{40}Ar on ^{238}U at $E_{lab}=170.0$ MeV ($\theta_{cm}=165^\circ$ corresponds to 162.0° in the laboratory). The difference of the excitation probability between these two angles is small compared to the variation of the excitation probability with spin and therefore excitation probabilities at 180° are useful to interpret experimental results at backward scattering angles (which are usually not results corresponding to exactly 180° because of experimental reasons).

If the projectile moves in on the target with zero initial impact parameter, then classically the collision takes place in a plane (defined by the projectile and the symmetry axis of the target), and only two degrees of freedom are relevant. In this case therefore, one can use the USCA method to

solve a much simpler planar problem and then, by properly weighting the probability amplitudes, obtain the backward scattering excitation probabilities for the 3-dimensional problem.

a) Equations of motion.

Let the z-axis be the initial beam axis and let θ, β be the azimuthal angle of the projectile and the symmetry axis of the target, respectively. It is convenient to introduce the angles (see Fig. 1)

$$\chi \equiv \beta - \theta \tag{3a}$$

$$\gamma \equiv \beta + \theta \tag{3b}$$

If r is the distance between the nuclear centers and p_r, p_χ, p_γ are the canonically conjugate momenta to the generalized coordinates r, χ, γ then we can write the classical Hamiltonian for the system as:

$$H(r,\chi;p_r,p_\chi) = \frac{p_r^2}{2m} + p_\chi^2\left(\frac{1}{2mr^2} + \frac{1}{2\mathcal{I}}\right) + \frac{Z_T Z_p e^2}{r} + \frac{Z_p e^2 Q_0^{(2)}}{2r^3} P_2(\cos\chi) \tag{4}$$

Here we have explicitly made use of the fact that $\ell_{in}=0$ and that initially the rotational angular momentum of the target is zero (ground state of an even-even nucleus), i.e. that the total angular momentum J=0 and this implies that $p_\gamma(t)=0$. In the ex-

pression for the Hamiltonian m is the reduced mass of the target-projectile system, $\mathcal{I}$ is the nuclear moment of inertia of the target, Z_T, Z_P are the charge numbers of the target and projectile respectively and $Q_o^{(2)}$ is the intrinsic quadrupole moment of the target. This Hamiltonian does not take into account any interaction between the target and the projectile due to the nuclear force nor any higher electric and magnetic multipole moments. Also we are not taking into account any excitation of the projectile nor any excitation of the target besides the excitation of the collective rotational degree of freedom. The electric intrinsic quadrupole moment $Q_o^{(2)}$ is defined by:

$$Q_o^{(2)} = \sqrt{\frac{16\pi}{5}} \frac{q_{20}}{e} \tag{5}$$

with

$$q_{\lambda\mu} = \int d^3r \, \rho(\underset{\sim}{r}) Y_{\lambda\mu}(\hat{r}) r^\lambda \tag{6}$$

where $\rho(\underset{\sim}{r})$ is the charge density of the target.

The Hamiltonian depends only on two coordinates and their canonical conjugate momenta. The four equations of motion are:

$$\dot{r} = \frac{p_r}{m} \tag{7a}$$

$$\dot{p}_r = \frac{p_\chi^2}{m r^3} + \frac{Z_p Z_T e^2}{r^2} + \frac{3 Z_p e^2 Q_o^{(2)}}{2 r^4} P_2(\cos\chi) \tag{7b}$$

$$\dot{\chi} = \left(\frac{1}{m r^2} + \frac{1}{\mathcal{I}} \right) P_\chi \tag{7c}$$

$$\dot{P}_\chi = - \frac{Z_p e^2 Q_0^{(2)}}{2 r^3} \frac{\partial}{\partial \chi} P_2(\cos\chi) \tag{7d}$$

If one is interested in the angles β and θ, then the value of γ has to be known, which can be found by integrating

$$\dot{\gamma} = \left(- \frac{1}{m r^2} + \frac{1}{\mathcal{I}} \right) P_\chi \tag{7e}$$

Another quantity of interest is the phase Φ which is in this case:

$$\Phi = - \frac{1}{\hbar} \int_{t_i}^{t_f} \left(r \dot{P}_r + \chi \dot{P}_\chi \right) dt \tag{8}$$

The differential equation for Φ is therefore

$$\dot{\Phi} = - \frac{1}{\hbar} \left(r \dot{P}_r + \chi \dot{P}_\chi \right) \tag{9}$$

The eqs. (7) are integrated numerically with the initial conditions:

$$r_i = \text{large} \tag{9a}$$

$$\dot{P}_{r_i} = \sqrt{2m\left(E_{cm} - \frac{Z_T Z_p e^2}{r_i}\right)} \tag{9b}$$

$$\chi_i = \beta_0 \quad (\text{arbitrary}) \tag{9c}$$

$$P_{\chi_i} = 0 \tag{9d}$$

$$\gamma_i = \beta_0 \tag{9e}$$

$$\Phi_i = 0 \tag{9f}$$

The initial distance, r_i, was taken to be 20 times the distance of closest approach. The quantity p_χ is the classical angular momentum of the target; the rotational energy of the planar rotor is given (classically) by:

$$E = \frac{P_\chi^2}{2\mathcal{I}} \tag{10}$$

One of the advantages of this orbital method is the ease of including other terms in the interaction potential. In some cases a hexadecapole potential

$$V_{Hexa} = \frac{Z_p e^2 Q_0^{(4)}}{2r^5} P_4(\cos\chi) \tag{11}$$

was used where $Q_o^{(4)}$ is defined by:

$$Q_o^{(4)} = \sqrt{\frac{16\pi}{9}}\ \frac{q_{40}}{e} \qquad (12)$$

For energies below the Coulomb barrier it is also easy to include the exponential tail of the real nuclear potential and so get the nuclear-Coulomb interference in this case. However, when the energy is above or close the barrier top, the complete nuclear potential has to be used. The orbital method for complex potentials (with complex trajectories) was recently applied to heavy ion elastic and inelastic scattering [6, 7].

b) Excitation Probability.

Integrating the equations of motion with the initial condition $\chi = \beta_o$ for various values of β_o, the "quantum number" function $\hat{I}(\beta_o)$ is found, where $\hat{I}$ is the value of p_χ after the integration.

The target nucleus has, besides the azimuthal symmetry, also a reflection symmetry. This symmetry has as a consequence that only even spins I can be excited and one needs to consider only roots in the interval $[0, \pi/2]$; also in the expression for the S matrix the factor $8/i\pi$ instead of $1/2i\pi$ appears in the preexponential factor.

For $I \leqslant I_{max}$ one has two real roots to the equation

$$\hat{I}(\beta_o) = I \qquad (13)$$

in the interval $[0, \pi/2]$. Let's call the two roots β_1 and β_2. The S matrix is then:

$$S = \sqrt{-\frac{8}{\pi i}\left(\frac{\partial^2\Phi}{\partial I_i \partial I_f}\right)_1}\, e^{i\Phi_1} + \sqrt{-\frac{8}{\pi i}\left(\frac{\partial^2\Phi}{\partial I_i \partial I_f}\right)_2}\, e^{i\Phi_2} \qquad (14)$$

where Φ is given by (2). Writing it in a different form:

$$\Phi = -\frac{1}{\hbar}\int_{I_i}^{I_f}\left(r\frac{\partial p_r}{\partial I} + \hbar\chi\right) dI \qquad (15)$$

Using

$$\frac{\partial\Phi}{\partial I_i} = \chi_i = \beta_0 \qquad (16)$$

and introducing the definitions

$$P_1 \equiv \frac{4\left(1-\frac{1}{2}\delta_{I0}\right)}{\pi\left|\left(\frac{\partial I}{\partial\beta_0}\right)_1\right|} \qquad (17)$$

$$s_1 \equiv \operatorname{sgn}\left(\left(\frac{\partial I}{\partial\beta_0}\right)_1\right) \qquad (18)$$

(and similarly for root 2) one can write the S matrix in a more useful form:

$$S_{0I}(E) = \sqrt{P_1}\, e^{i\left(\Phi_1 + \frac{\pi}{4}s_1\right)} + \sqrt{P_2}\, e^{i\left(\Phi_2 + \frac{\pi}{4}s_2\right)} \qquad (19)$$

The factor $(1-\delta_{I0}/2)$ appears in eq. (17) because the "phase space" of initial orientations leading to I=0 is half as large than for $I \neq 0$.

The square of this S matrix can be interpreted as an excitation probability for backward scattering angles, so we have what is called the primitive semiclassical expression:

$$P_{sc}(I) = \left| S_{oI}(E) \right|^2$$

$$= \left(P_1 + P_2 + 2\sqrt{P_1 P_2} \sin(\Delta\Phi) \right) \qquad (20)$$

where

$$\Delta\Phi \equiv \left| \Phi_1 - \Phi_2 \right| \qquad (21)$$

The USCA method can also be used to obtain excitation probabilities to final states with $I > I_{max}$ [2,3]. For $I > I_{max}$ there are two complex solutions (one conjugate to the other) to the equation $\hat{I}(\beta_o)=I$, also the two phases Φ_1 and Φ_2 become complex conjugate of each other.

$$\Phi_1 = \Phi_R + i\,\Phi_I \qquad \text{with} \quad \Phi_I \geq 0$$

$$\Phi_2 = \Phi_1^* \qquad (22)$$

Let's note that root 1 is defined as the one with positive

imaginary phase. The S matrix in this case is:

$$S = \frac{e^{i\Phi_R}\, e^{-\Phi_I}}{\sqrt{\frac{\pi}{2i}\left(\frac{\partial I}{\partial \beta_0}\right)_1}} \qquad (23)$$

Only one root contributes to the S matrix. If the other root were present one would have a contribution from that root which is exponentially increasing with I, which is unacceptable from physical grounds.

For the excitation probability we find

$$P_{sc} = P_1 e^{-2\Phi_I} \qquad (24)$$

c) Uniform Semiclassical Expressions

For I close to I_{max} the equations (20) and (23) do not represent at all a good approximation to the excitation probability (one has $\partial I/\partial\beta \to 0$ and p_1 and $p_2 \longrightarrow \infty$). The origin of this difficulty lies in the fact that in this case the two roots β_1, β_2 become very close and then the evaluation of the integrals, in the derivation of the equations of section II, by the stationary phase approximation has to be modified. This difficulty disappears when the so called uniform semiclassical expressions are used:

$$P_{uni} = \pi\sqrt{z}\left\{\left(\sqrt{P_1}+\sqrt{P_2}\right)^2 Ai^2(-z) + \left(\sqrt{P_1}-\sqrt{P_2}\right)^2 Bi^2(-z)\right\} \qquad (25)$$

$$I \leq I_{max}$$

and

$$P_{uni} = 4\pi\sqrt{z}\,P_1\,Ai^2(z) \qquad I > I_{max} \qquad (26)$$

where Ai and Bi are the Airy functions, and z is given by:

$$z = \left(\frac{3}{4}\,\Delta\Phi\right)^{2/3} \qquad (27)$$

A rigorous derivation of these equations is possible [2]. Using the asymptotic expression for the Airy functions one can show that eqs. (25) and (26) approach eqs. (20) and (23) when $|I|$ is not close to I_{max}.

Equation (26) is not easily applied. To obtain $\Delta\Phi$ without integrating the equations of motion with complex variables one has to approximate $\hat{I}(\beta)$ as a quadratic and Φ as a cubic about β_{max} and this leads to the equation [2]:

$$P_{uni} \simeq 4\,\frac{Ai^2\left(\frac{\Delta I}{A}\right)}{A^2\left|\frac{\partial \bar{x}_f}{\partial \beta_0}\right|} \qquad (28)$$

with

$$\Delta I = |I| - I_{max} \qquad (29)$$

$$A = \frac{\left(\partial^2 I_f/\partial\beta_0^2\right)_{max}}{2\left(\partial \bar{x}_f/\partial\beta_0\right)^2_{max}} \qquad (30)$$

$$\overline{\chi}_f \equiv -\frac{\partial \Phi}{\partial I_f} = -\frac{m\hbar}{\mathcal{I}}\left(\frac{\vdash I}{P_\vdash}\right)_f + \chi_f \qquad (31)$$

d) Modifications for three-dimensional backscattering

So far the problem considered has been the backscattering from a rotor in two dimensions (2D). Here we would like to modify the previous equations so that they correspond to the three dimensional (3D) backscattering from a rotor, without integrating the full three dimensional equations of motion.

The energy levels of a quantum mechanical rotor in 3D are given by:

$$E_I = \frac{\hbar^2}{2\mathcal{I}}(I+1)I \qquad (32)$$

Using equation (10) one would like to make the identification $p_\chi = \hbar\sqrt{I(I+1)}$, however, since $p_\chi/\hbar$ is the action variable in this case, it has to vary by an integer for the various states of the system (see section II). The next best suggestion, and the one adopted here, is to make the usual semiclassical identification:

$$P_\chi = \hbar(I+1/2) \qquad (33)$$

which also gives the correct energy spacings when using equation

(10). We solve therefore (in the 3D case) for roots of the function $\hat{I}(\beta_0)$ at even integers plus 1/2.

The moment of inertia is obtained from the experimental energy of the first excited rotational state of the target E_2 and eq.(32), that is

$$\mathcal{I} = \frac{3\hbar^2}{E_2} \tag{34}$$

Figure 2 shows a typical graph of the function $\hat{I}(\beta_0)$. At 0° and 90° $\hat{I}(\beta_0)$ goes trough zero since in those cases no torque acts on the target, and we are assuming that initially the target is not rotating. How to modify the p's (defined in eq. (17)) can be deduced by noting that for $I \neq 0$

$$P_1 \equiv \frac{2}{\frac{\pi}{2}\left|\left(\frac{\partial I}{\partial \beta_0}\right)_1\right|} \simeq \frac{|\beta_1^< - \beta_1^>|}{\pi/2} \tag{35}$$

i.e. p_1 has the geometrical meaning that it is the probability that the initial orientation of the (2D) rotor is in the interval $[\beta_1^<, \beta_1^>]$, ($\beta_1^<$ and $\beta_1^>$ are defined in Fig. 2). Defining $\bar{p}_1$ as the probability that the initial azimuthal angle of a rotor in three dimensions is in the interval $[\beta_1^<, \beta_1^>]$ we find:

$$\bar{P}_1 = \frac{2\pi \sin\beta_1 \, |\beta_1^< - \beta_1^>|}{2\pi} = \frac{2\sin\beta_1}{\left|\left(\frac{\partial I}{\partial \beta_0}\right)_1\right|} \tag{36}$$

The $\sin\beta_1$ factor arises from a purely geometrical argument (see Fig. 3). The excitation probabilities for the 3D backscattering problem are obtained when in the previous expressions the p's are replaced by the $\bar{p}$'s.

To be able to make the above argument it is necessary for the target not to rotate (in the plane where the scattering is going to take place) initially and therefore one still integrates the equations of motion with the initial condition $p_\chi = 0$. It is not very clear whether this is really inconsistent with eq.(33) since the equations of motion we integrate belong to a rotor in two dimensions and a rotor in two dimensions does not have the energy levels given by eq.(32). For I=0 one has to multiply $\bar{p}$ by 0.75 since the initial orientations space leading to I=0 is 25% smaller then for $I \neq 0$ (see Fig.2).

The prescription described in this section is the one followed in this paper and is the one giving the most consistent results when comparing to the De Boer - Winther code (where the "internal" degrees of freedom are treated quantum mechanically). This prescription is far better than using instead of eq.(33) the identification $p_\chi = \hbar I$.

IV Results and Discussion

a) Examples.

For a typical case, $^{40}Ar + ^{238}U$ at $E_{lab} = 170.0$ MeV (without hexadecapole nor nuclear interaction) the function $\hat{I}(\beta_0)$ and $\Phi(\beta_0)$ obtained by integrating the equations of motion are shown in Fig. 4. The function $\hat{I}(\beta_0)$ is periodic with period of $\pi/2$ since the force from a monopole-quadrupole potential has this periodicity. The phase Φ, however, does not have this property (it is not periodic with any period).

In our code the functions $\hat{I}(\beta_0)$ and $\Phi(\beta_0)$ were computed with an interval of 5°. We use a simple three-point quadratic interpolation between the discrete points to find the roots of the equation $\hat{I}(\beta_0) = I + 1/2$. Calling β_1, β_2 the roots for I+1/2 and β_3, β_4 the roots for $-(I+1/2)$, then one finds that $\Delta\Phi = |\beta_1 - \beta_2| = |\beta_3 - \beta_4|$, i.e. even though the function Φ is quite different in the intervals $[0, \pi/2]$ and $[\pi/2, \pi]$, the phase difference for a given final state is the same in both intervals. This justifies restricting oneself to the interval $[0, \pi/2]$. The derivatives $(\partial I/\partial\beta_0)_k$ (and therefore $\bar{p}_k$) are also immediately found by using the fitting coefficients of the function $\hat{I}(\beta_0)$.

In Fig. 5 $\Delta\Phi$ and $\sqrt{\bar{p}}$ are plotted vs. I. Fig. 6 shows the excitation amplitude for this example calculated in different ways. First of all there is the classical excitation probability

$P_{cl} = \bar{p}_1 + \bar{p}_2$, which has no interference effect and goes only up to spin $I = 8$ since this is the largest spin allowed by classical dynamics (see Fig. 4). For $I = 0$ the excitation probability is roughly $3/4$ of what it is for $I = 2$; this is not an interference effect but rather has to do with the fact that the space of initial orientations leading to $I = 0$ is about $3/4$ as large as the one leading to $I = 2$ (see Fig. 2). The uniform semiclassical result in three dimensions (that is eq. (25) and (26) but with the $\bar{p}$'s instead of the p's) is indicated by open circles in Fig. 6 . For comparison the result using the semiclassical code for multiple Coulomb excitation of De Boer - Winther is also indicated. The agreement is very reasonable.

The main features of the 3D-USCA can be understood by using Fig. 5 and remembering that the primitive semiclassical expression should give similar results to the uniform semiclassical, except when I is close to I_{max} (in our example $I \sim 10$). The regions where the interference is constructive or destructive are indicated in Fig. 5 . For $I = 4$, for example, $\Delta\Phi$ is in a region of destructive interference. Hence, P_{uni} is much smaller then P_{cl}. For $I = 6$, $\Delta\Phi$ is only slightly into a region of constructive interference, therefore P_{uni} is a little larger then P_{cl}. The fact that $\sqrt{\bar{p}_1}$ goes to zero for small $I+1/2$ in the 3D case (due to the $\sin\beta_1$ in eq. (36)) has the consequence that the interference pattern becomes progressively weaker going to small I . In the 2D-USCA $\sqrt{p_1}$ does not tend to zero (as a matter fact the curves for $\sqrt{p_1}$ and $\sqrt{p_2}$ are fairly similar and lie between the curves

$\sqrt{\bar{p}_1}$ and $\sqrt{\bar{p}_2}$ of Fig. 5); and therefore the 2D interference pattern is much larger (see Fig. 6), in disagreement with the De Boer - Winther code.

In our example the excitation probabilities add up to unity (to within a fraction of 1%) as required by the unitarity of the S matrix.

We would note at this point that we have recently learned of a similar independent treatment of Coulomb excitation by Levit, Smilansky and Pelte[8]. There are some differences between the formulations, such as, (1) they do not make the $\sin\beta$ weighting to go to the three dimensional application, i.e. they solve the backscattering from a planar rotor, (2) they neglect the transverse force term in the equations of motion, so as to constrain the orbit exactly to the beam axis (this effect is actually very small).

In Fig. 7 we show the excitation probability for the same example at a higher energy (E_{lab}=200.0 MeV), with and without hexadecapole potential. Again we find the same kind of agreement with the De Boer-Winther code. The excitation probability with $Q_o^{(4)} \neq 0$ falls off ~~slower~~ more slowly for large I than with $Q_o^{(4)}=0$. In our case this comes about because the function $\hat{I}(\beta_o)$ is flatter at the maximum when $Q_o^{(4)} \neq 0$.

The main difference between the results computed with the De Boer-Winther and our code are the smaller excitation amplitudes we find for large I. Large spins are excited when the initial azimuthal angle of the target is around 34° (see Fig. 4).

The quadrupole potential at this orientation exerts a repulsive force on the projectile; the projectile therefore does not come as close to the target and spends less time there than if it were moving in a pure Coulomb trajectory and as a consequence high I states are less excited than calculated with the De Boer-Winther code. However, an estimate of this effect shows that it should be much smaller than the one shown in Figs. 6 and 7. There are several possible reasons to explain this difference: (1) In the evaluation of excitation probabilities for "classically forbidden" transitions (that is, transitions to states not reached by classical dynamics) we are using the approximate formula (28) instead of equation (26); (2) we are approximating the extremum of the function $\hat{I}(\beta_0)$ (which occurs around 34° for our example; see Fig. 2) by a parabola, an approximation which may not be too good for (classically) very forbidden transitions; (3) the transition from 2D to 3D (as outlined in III-d) may not be quite consistent; (4) since a fully quantum mechanical calculation is not available for comparison, we do not know the actual errors in either the De Boer - Winther calculation or the uniform semiclassical.

b) The Limit of Sudden Collision.

In this section we will limit the discussion only to quadrupole Coulomb excitation.

When writing the equations of motion (7) in terms of dimensionless quantities one finds that the evolution of the system depends only on the following dimensionless parameters:

$$\eta = \frac{Z_T Z_p e^2}{\hbar v_0} \qquad \text{(Sommerfeld parameter)} \qquad (37a)$$

$$\xi_{02} = \eta \frac{E_2}{2 E_{cm}} \qquad \text{(Adiabaticity parameter)} \qquad (37b)$$

$$\bar{q}_2 = \frac{Z_p e^2 Q_0^{(2)}}{4 \hbar v_0 a^2} \qquad \text{(Quadrupole interaction strenght parameter)} \qquad (37c)$$

where v_0 is the velocity of the incoming projectile and $\underline{a}$ is half the distance of closest approach:

$$a = \frac{Z_p Z_T e^2}{2 E_{cm}} \qquad (38)$$

In order to limit the number of parameters (and so make the comparison with the conventional semiclassical method easier) we consider from now on the case $\xi_{02} = 0$. This corresponds physically to the limit of sudden collision (that is, the period of rotation of the target is much larger than the time during which the interaction takes place). For the conventional semiclassical approach, this $\xi_{02} = 0$ limit has been studied by Alder and Winther [10], and one has there that the excitation probability for backscattering depends only on the quadrupole interaction strength $\bar{q}_2$. In our case, however, we have also the additional parameter η, $\bar{q}_2/\eta$ giving a measure of how much the orbit of the projectile is disturbed by the interaction. The conventional semi-

classical method corresponds therefore to $\eta \to \infty$. It can be shown [9] that classically the largest azimuthal angle θ through which the projectile can be scattered is approximately $2\bar{q}_2/\eta$.

A nice feature of the USCA method is that the $\xi_{20} = 0$, $\eta \to \infty$ limit for backscattering can be solved analytically. The result for the function $\hat{I}(\beta_0)$ and $\Phi(\beta_0)$ is

$$\hat{I}(\beta) = 2\bar{q}_2 \sin(2\beta) \tag{39}$$

$$\Phi(\beta) = 2\bar{q}_2 \left(\sin^2\beta - \beta \sin(2\beta) \right) \tag{40}$$

from which the phase difference $\Delta\Phi$ and the $\bar{p}$'s can be found:

$$\Delta\Phi = \begin{cases} 2\bar{q}_2 \left| \sqrt{1-f^2} - f \operatorname{Arccos} f \right| & f \leq 1 \\ 2\bar{q}_2 \left| \sqrt{f^2-1} - f \operatorname{Log}\left(f + \sqrt{f^2-1}\right) \right| & f \geq 1 \end{cases} \tag{41}$$

$$\left.\begin{matrix} \bar{P}_1 \\ \bar{P}_2 \end{matrix}\right\} = \left(1 - \frac{\delta_{10}}{4}\right) \frac{1}{\bar{q}_2 \sqrt{1-f^2}} \begin{cases} \sin\left(\frac{\operatorname{Arcsin} f}{2}\right) \\ \cos\left(\frac{\operatorname{Arcsin} f}{2}\right) \end{cases} \quad f<1 \tag{42a}$$

$$\bar{P}_1 = \frac{1}{\sqrt{2}\,\bar{q}_2 \sqrt{f^2-1}} \qquad f>1 \tag{42b}$$

with f defined by:

$$f = \frac{I + 1/2}{2\bar{q}_2} \qquad (43)$$

In Fig. 8 the phase difference $\Delta\Phi$ vs. $\bar{q}_2$ is plotted for $f<1$. The regions of constructive and destructive interference are also indicated. With this figure one readily understands the features of the excitation probability (Fig. 7, ref. 10).

Substituting eqs. (41) and (42) back into eqs. (25) and (26) we find the excitation probabilities in the $\xi_{02} = 0$, $\eta \longrightarrow \infty$ limit. Let's note that in this case we are using the "exact" expression (26) for the classical forbidden transitions (that is for $f>1$) and not the approximate expression (28). For the special case $f = 1$ the excitation probability is:

$$P_{uni} = \frac{\pi}{\sqrt{2}} \left(\frac{2}{\bar{q}_2} \right)^{2/3} Ai^2(0) \qquad (44)$$

In Table II the excitation probabilities are tabulated for some values of I and compared with results tabulated by Alder and Winther (Table 5, ref. 10). Except for $I = 0$, where the difference is a little larger, the results are very similar, especially for large $\bar{q}_2$. The difference between the excitation probabilities calculated by the two different semiclassical methods (for not too small $\bar{q}_2$) is $\Delta P = P_{uni} - P_{sc}^{AW} \lesssim 0.003$. The results are tabulated since in a figure like Fig. 7 of reference 10 one would hardly find any difference between the two calcula-

culations. The agreement is very good even for small $\bar{q}_2$ ($\bar{q}_2 < 3$) where the uniform approximation with Airy functions should become gradually worse and a uniform expression in terms of Bessel functions should be applied [3]. For $\eta \to \infty$, the conventional semiclassical method and the quantum mechanical theory should give identical results; however, Table 5 in reference 10 was obtained with the use of some additional approximations and it is difficult to say whether the small differences between the two semiclassical calculations are due to (1) this additional approximation, (2) to the numerical evaluation of the excitation probabilities or (3) due to the basic approximations of the USCA method.

In realistic scattering problems, η is finite and the projectile's orbit will differ from a pure hyperbola, the quantity $\bar{q}_2/\eta$ being a measure of the size of the correction expected. Fig. 9 shows the $(\eta, \bar{q}_2)$ values for various target-projectile systems at several energies (in MeV). Figure 10 shows the backscattering excitation probability for $\xi_{02} = 0$ and $\bar{q}_2 = 9.$ vs. $1/\eta$. In our calculations one finds that by varying η from 50 to 350, the phase difference $\Delta\Phi$ increases for the various states between 0.3 and 0.7 radians; with this fact and Fig. 8 we can rationalize the variation of the excitation probability with η in Fig. 10. For example for $I = 6$, $\Delta\Phi$ moves away from the region of constructive interference with increasing η, therefore the excitation probability decreases; for $I = 8$, $\Delta\Phi$ moves

into a region of constructive interference, the excitation probability increases with η. The variation of $\Delta\Phi$ with η is the main contribution to the change in the excitation probability with η; the $\bar{p}$'s also vary with η (the larger the spin I, the greater the variation). For $I = 14$, $\Delta\Phi$ moves deeper into the constructive interference region and the excitation probability should increase with η, but this is cancelled by the decrease of the $\bar{p}$'s with increasing η, so the excitation probability actually goes down a little.

We should note here that in the De Boer - Winther code one takes approximately into account the energy loss of the projectile during the collision by choosing properly symmetrized orbits. In other words, some part of the corrections to the hyperbolic orbit due to the monopole - quadrupole interaction are taken into account. In the $\xi_{02} = 0$ case however, there is no energy loss and therefore the finite η corrections shown in Fig. 10 come about because of the change in the projectile's orbit due to the angular momentum transfer between the target and projectile. The angular momentum transfer between target and projectile is not taken into account in the conventional De Boer - Winther code although work is currently being done to include it approximately [4].

c) Conclusions.

The basic approach of the USCA is that one employs classical dynamics (equations of motion) but retains the quantum me-

chanical superposition principle (addition of probability amplitudes for indistinguishible processes rather than probabilities themselves). With these basic features one finds even a quantitative agreement with more conventional methods.

It is suggested that one could even get the corrections to the excitation probabilities in the De Boer - Winther code due to the coupling of the excitation process of the target and the orbital motion of the projectile.

The USCA can lead to a better explanation and gives more physical insight to the process as compared to the conventional semiclassical and quantum mechanical approach. Another advantage of this method is that the amount of computer time needed is practically independent of the number of final states considered (actually the more states that are excited the more applicable is the method).

If one wants results not only for backscattering, then one has to solve the full 3D problem. A full 3D calculation for Coulomb excitation is considerably more complicated to do; there one has two coordinates to specify the initial orientation of the target and one has to do a two dimensional root search to find the initial orientations leading to a given final state. In general there will be four roots; a uniform expression for four roots has been made plausible although it has not been proved rigorously [11].

We appreciate the help and many discussions we had with Mr. Larry Sterna during the developement of the computer code. We are also very indebted to Prof. Bill Miller for valuable discussions and suggestions. We would also like to thank Drs. Chin Fu Tsang and P. Colombani for comenting on the manuscript.

References

1) W. H. Miller, J. Chem. Phys. 53, (1970), 1949

2) W. H. Miller, J. Chem. Phys. 53, (1970), 3578

3) W. H. Miller, "The classical S-matrix in molecular collisions" in Molecular Beams, ed. K. P. Lawley, Wiley; to be published (1975).

4) J. De Boer and H. Massmann, unpublished.

5) J. De Boer and Aa. Winther, in Coulomb Excitation ed. by K. Alder and Aa. Winther, Academic Press (1966).

6) R. A. Malfliet; "Semiclassical description of Elastic and Inelastic Heavy Ion Scattering" invited talk at symposium on "Classical and Quantum Mechanical Aspects of Heavy Ion Collision". Heidelberg, Oct. 1974.

7) J. Knoll and R. Schaeffer, "Semiclassical Approximation for Complex potentials" Extended Seminar on Nuclear Physics, I.C.T.P. TRieste, (1973).
J. Knoll and R, Schaeffer "Semiclassical Approximation with Complex Potential" (submitted to "Physics Letters").

8) S. Levit, U. Smilansky and D. Pelte; "A new Semiclassical Theory for Multiple Coulomb Excitation". (Weizman Institute preprint).

9) N. Rowley and P. Colombany; "A classical description of the Coulomb Excitation of very Heavy Deformed Nuclei"; Submitted to "Physical Review" (Orsay preprint).

10) K. Alder and Aa. Winther, Kgl. Danske Videnskab. Selskab, Mat. Fys. Medd. 32 Nr. 8, (1960).

11) W. H. Miller, J. Chem. Phys. 54, (1971), 5386.

*) Work supported by the U. S. Energy Research and Developement Administration.

**) On leave from Facultad de Ciencias, U. de Chile, Santiago Chile, with a fellowship from Convenio U. de Chile - U. of California.

Table I

Probability to excite a rotational state of angular momentum I calculated with the De Boer-Winther code for $^{40}Ar+^{238}U$ at E_{lab}=170 MeV, $Q_o^{(2)}$=10.84 barn.

I	$\theta_{cm} = 180$	$\theta_{cm} = 165$
0	0.07859	0.08195
2	0.17013	0.16754
4	0.05372	0.05422
6	0.20703	0.22377
8	0.29012	0.28689
10	0.15091	0.14127
12	0.04146	0.03735
14	0.00716	0.00626
16	0.00088	0.00076

Table II

The probabilities for excitation of rotational states in an even-even nucleus in the limit $\xi_{02}=0$ and $\gamma=\infty$. Tabulated are the results of the USCA and the traditional semiclassical approximation (ref.9).

$\bar{q}_2$	USCA	A-W	USCA	A-W	USCA	A-W
	P_0	P_0	P_2	P_2	P_6	P_6
1.0	0.6339	0.6945	0.2518	0.2850	0.0003	0.0006
1.5	0.3830	0.4300	0.4917	0.4812	0.0039	0.0057
2.0	0.1940	0.2152	0.5733	0.5597	0.0203	0.0260
2.5	0.0988	0.1021	0.4892	0.4842	0.0650	0.0750
3.0	0.0842	0.0835	0.3084	0.3098	0.1485	0.1572
3.5	0.1067	0.1108	0.1362	0.1389	0.2568	0.2563
4.0	0.1224	0.1317	0.0509	0.0514	0.3385	0.3354
4.5	0.1115	0.1214	0.0622	0.0600	0.3571	0.3555
5.0	0.0820	0.0881	0.1193	0.1158	0.2999	0.3006
5.5	0.0553	0.0571	0.1569	0.1540	0.1911	0.1932
6.0	0.0461	0.0463	0.1427	0.1412	0.0828	0.0848
6.5	0.0530	0.0547	0.0921	0.0917	0.0242	0.0250
7.0	0.0630	0.0671	0.0462	0.0459	0.0317	0.0312
7.5	0.0637	0.0687	0.0352	0.0343	0.0809	0.0798
8.0	0.0532	0.0570	0.0568	0.0552	0.1251	0.1242
8.5	0.0396	0.0413	0.0836	0.0819	0.1293	0.1292
9.0	0.0324	0.0329	0.0892	0.0879	0.0925	0.0930
9.5	0.0345	0.0355	0.0692	0.0685	0.0442	0.0447
10.0	0.0409	0.0432	0.0412	0.0408	0.0188	0.0189

(to be continued)

Table II (continued)

$\bar{q}_2$	USCA	A-W	USCA	A-W	USCA	A-W
	P_{10}	P_{10}	P_{14}	P_{14}	P_{18}	P_{18}
1.0						
1.5						
2.0	0.0000	0.0001				
2.5	0.0004	0.0006				
3.0	0.0022	0.0029				
3.5	0.0084	0.0104		0.0001		
4.0	0.0247	0.0286	0.0003	0.0004		
4.5	0.0581	0.0634	0.0011	0.0014		
5.0	0.1127	0.1171	0.0038	0.0046		
5.5	0.1829	0.1831	0.0107	0.0124		0.0002
6.0	0.2451	0.2436	0.0255	0.0283	0.0006	0.0007
6.5	0.2768	0.2757	0.0523	0.0558	0.0018	0.0022
7.0	0.2615	0.2616	0.0933	0.0961	0.0050	0.0058
7.5	0.2004	0.2014	0.1452	0.1455	0.0120	0.0134
8.0	0.1160	0.1174	0.1946	0.1938	0.0253	0.0274
8.5	0.0436	0.0446	0.2266	0.2258	0.0478	0.0503
9.0	0.0124	0.0128	0.2277	0.2275	0.0808	0.0828
9.5	0.0290	0.0286	0.1930	0.1935	0.1221	0.1223
10.0	0.0725	0.0719	0.1316	0.1326	0.1627	0.1622

Figure Captions

Fig. 1. Diagram showing the geometry for the projectile - target system.

Fig. 2. Graph of the function $\hat{I}(\beta)$ vs. β. The two roots β_1 and β_2 of $\hat{I}(\beta) = I + 1/2$ are shown for $I = 4$.

Fig. 3. Initial orientation of the target. The probability that the azimuthal angle of the symmetry axis lies between β_o and $\beta_o + d\beta_o$ is clearly proportional to $\sin\beta_o$ in the 3D case.

Fig. 4. Graphs of the function $\hat{I}(\beta)$ and $\Phi(\beta)$ are shown for the case $^{40}Ar + ^{238}U$ at $E_{lab} = 170.0$ MeV. For this example: $\bar{q}_2 = 5.574$, $\eta = 127.0$, $\xi_{o2} = 0.0196$.

Fig. 5. Graph of $\Delta\Phi$, $\sqrt{\bar{p}_1}$ and $\sqrt{\bar{p}_2}$ vs. I for the same example of Fig. 2.

Fig. 6. Calculations of Coulomb excitation probabilities to excite members of rotational ground band in ^{238}U with the back-scattering of ^{40}Ar at $E_{lab} = 170.0$ MeV on ^{238}U. For this case: $E_2 = 0.0449$ MeV, $Q_o^{(2)} = 10.84$ barn, $Q_o^{(4)} = 0.0$ barn^2, $\xi_{o2} = 0.0196$, $\eta = 127.0$ and $\bar{q}_2 = 5.574$.

Fig. 7. Calculation with the USCA-3D and the De Boer - Winther code of Coulomb excitation probabilities to excite members of the rotational ground band of ^{238}U with the backscattering ($\theta = 180^{\circ}$) of ^{40}Ar ($E_{lab} = 200.0$ MeV) on ^{238}U. For this case: $E_2 = 0.0449$ MeV, $Q_o^{(2)} = 10.84$ barn, $\xi_{o2} = 0.0153$, $\eta = 117.1$ and $\bar{q}_2 = 7.112$. Two cases are shown: with hexadecapole moment $Q_o^{(4)} = 2.65$ barn^2 and without hexadecapole moment ($Q_o^{(4)} = 0$).

Fig. 8 .Graph of phase difference $\Delta\Phi$ vs. $\bar{q}_2$ for the case $\xi_{o2} = 0$ and $\eta \longrightarrow \infty$, obtained with eq. (41). Shown are the results for all spins up to $I = 18$ but only for $f \leq 1$.

Fig. 9. The (η, $\bar{q}_2$) values for various target - projectile systems at several laboratory energies (in MeV) are shown. The cross (X) indicates the place where $2a = 1.4 (A_T^{1/3} + A_p^{1/3})$ ($\underline{a}$ is defined by eq. (38)).

Fig. 10. Backward scattering excitation probabilities to Coulomb excite members of a ground rotational band of an even-even target. Results are shown vs. η for $\xi_{o2} = 0$ and $\bar{q}_2 = 9.0$. The $\eta \longrightarrow \infty$ limit was evaluated in the way described in IV-b.

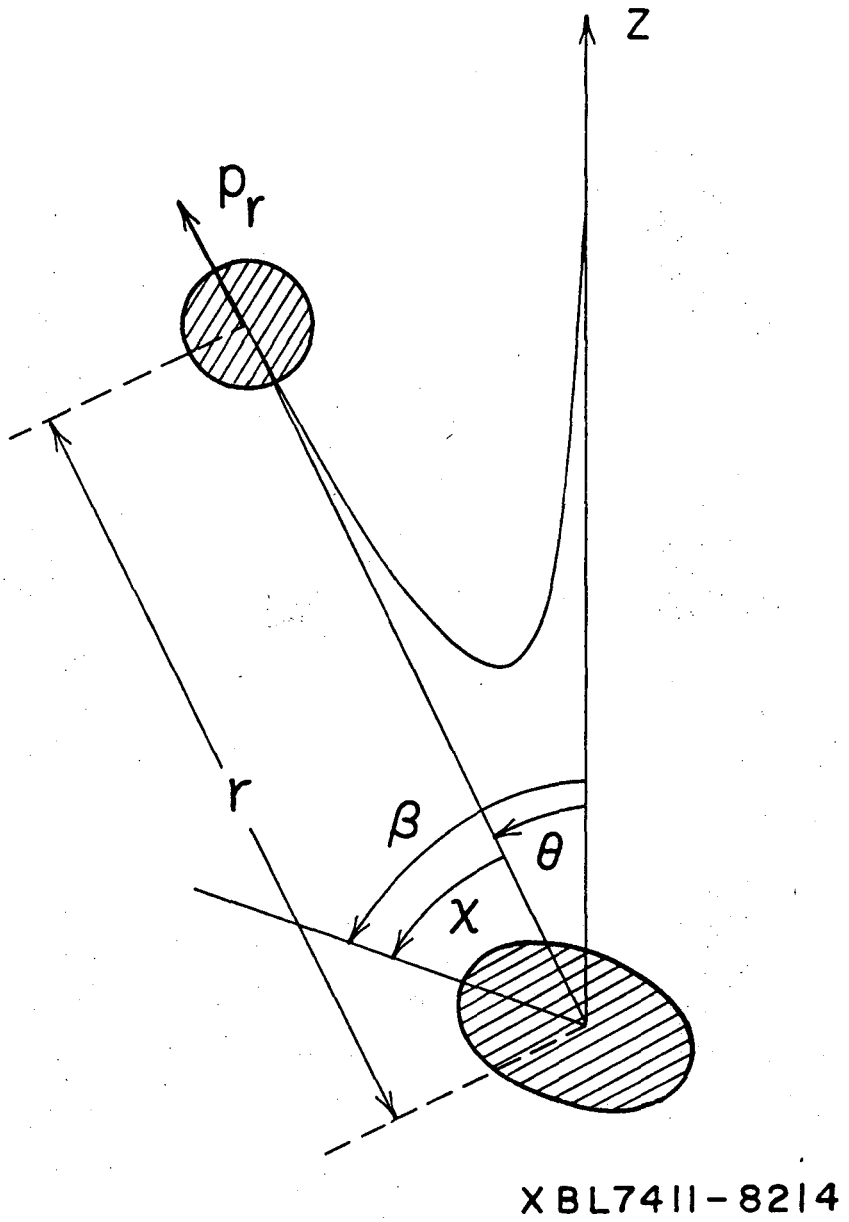

Fig. 1

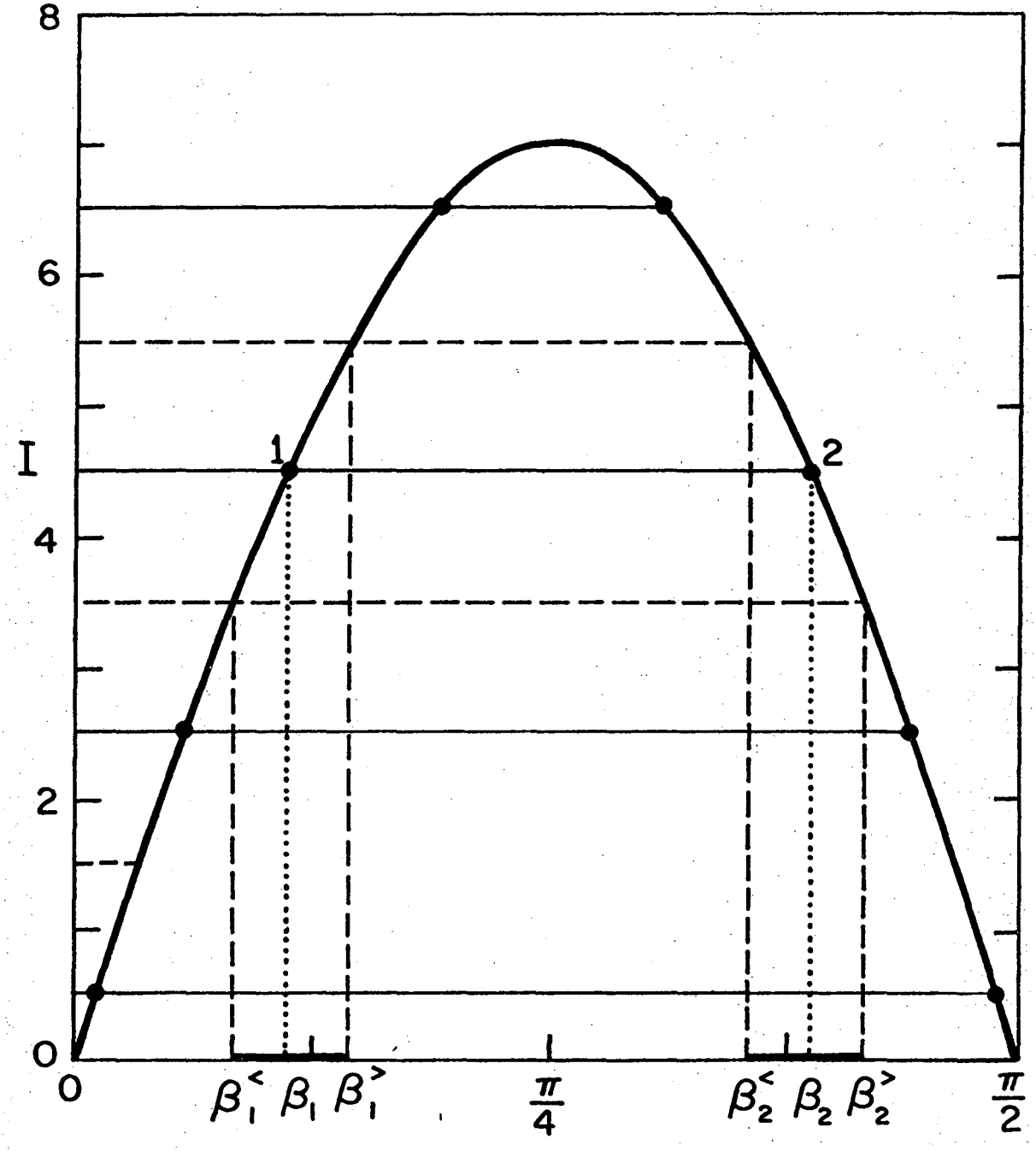
8
6
4
2
0
I
1
2
0
$\beta_1^<$ β_1 $\beta_1^>$
$\frac{\pi}{4}$
$\beta_2^<$ β_2 $\beta_2^>$
$\frac{\pi}{2}$
XBL7410-4541

Fig. 2

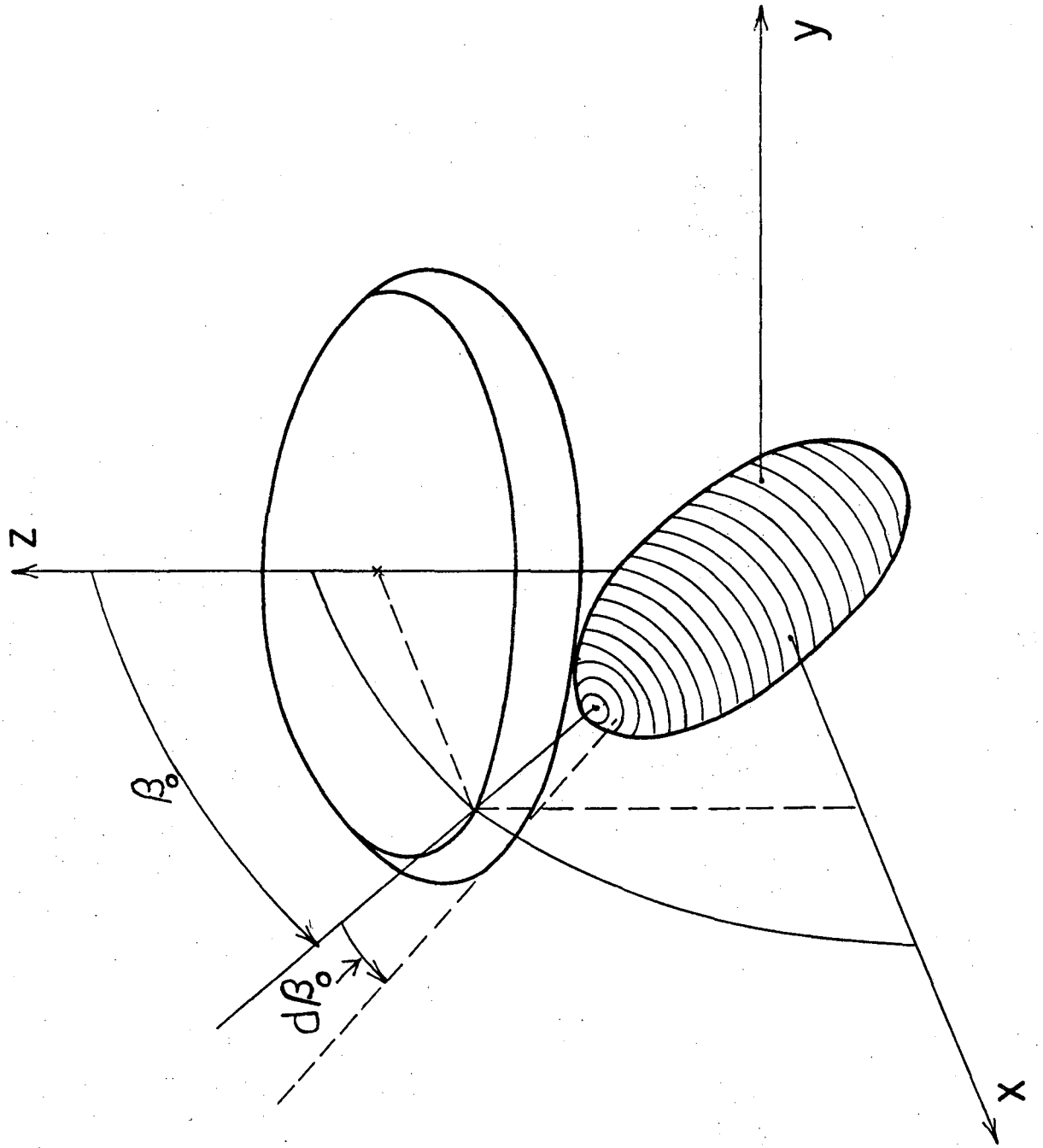

XBL7411-8213

Fig. 3

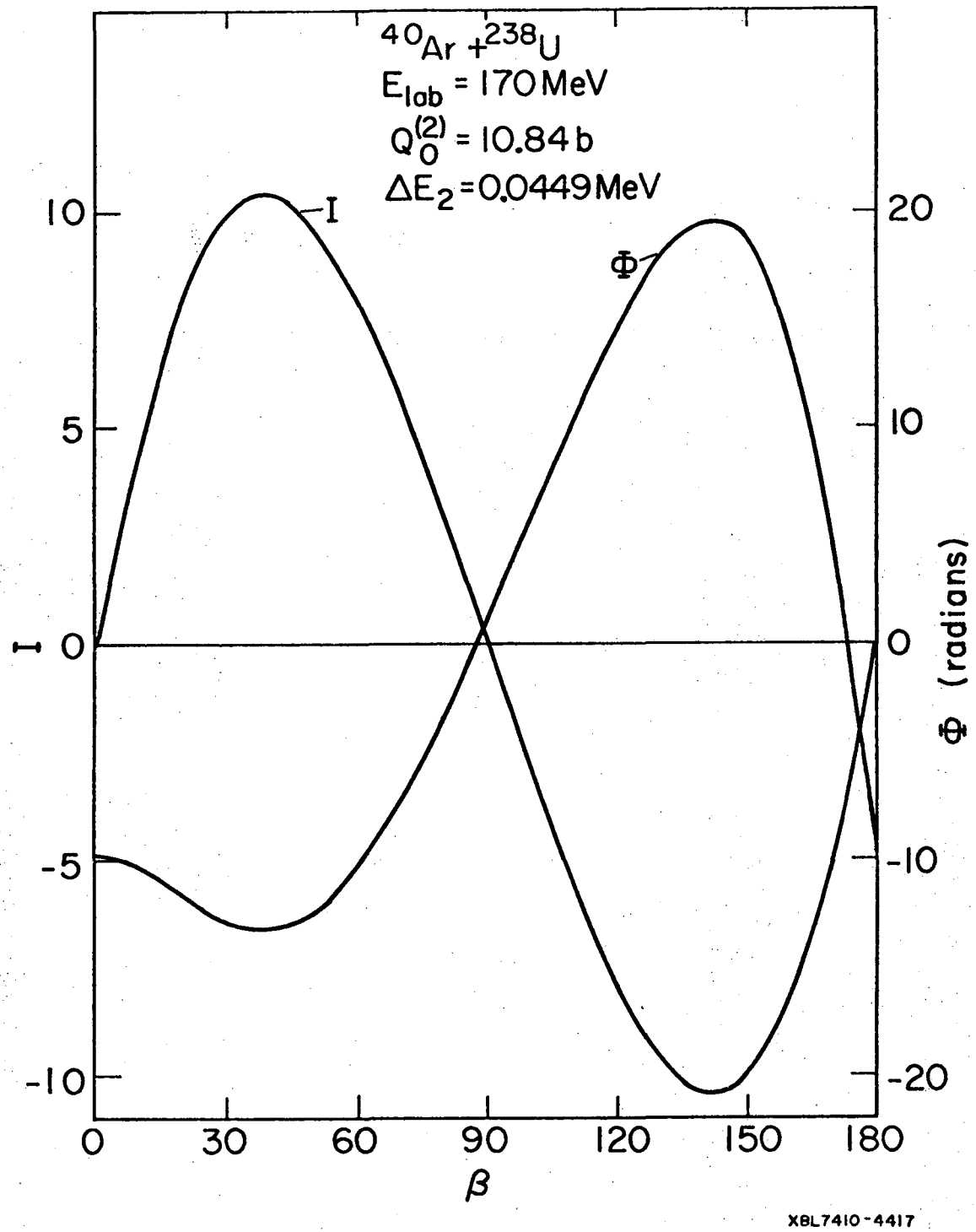
$^{40}Ar + ^{238}U$
E_{lab} = 170 MeV
$Q_0^{(2)}$ = 10.84 b
ΔE_2 = 0.0449 MeV
I
Φ
10
5
0
-5
-10
20
10
0
-10
-20
I
Φ (radians)
0
30
60
90
120
150
180
β
XBL7410-4417

Fig. 4

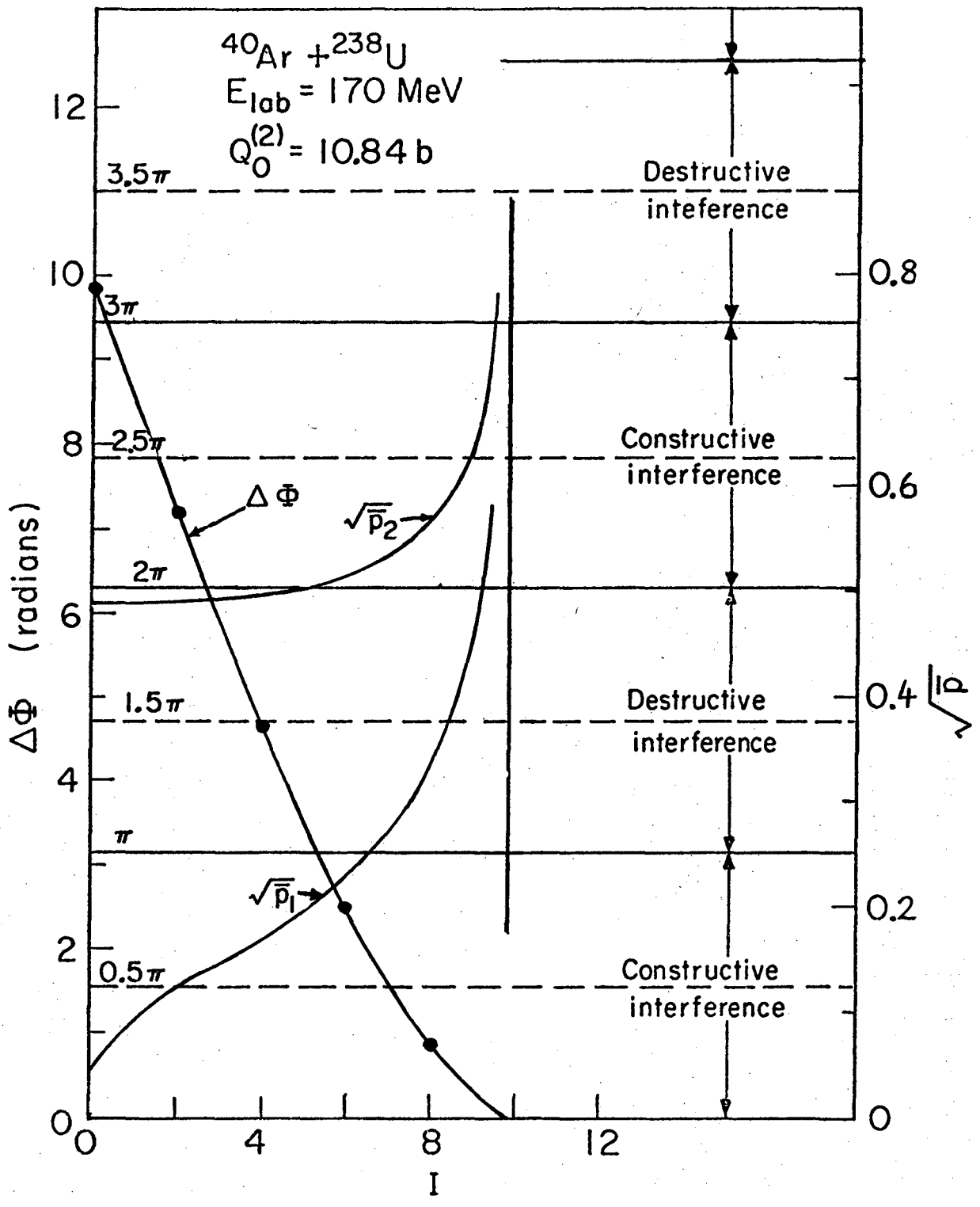

XBL 7410-4419A

Fig. 5

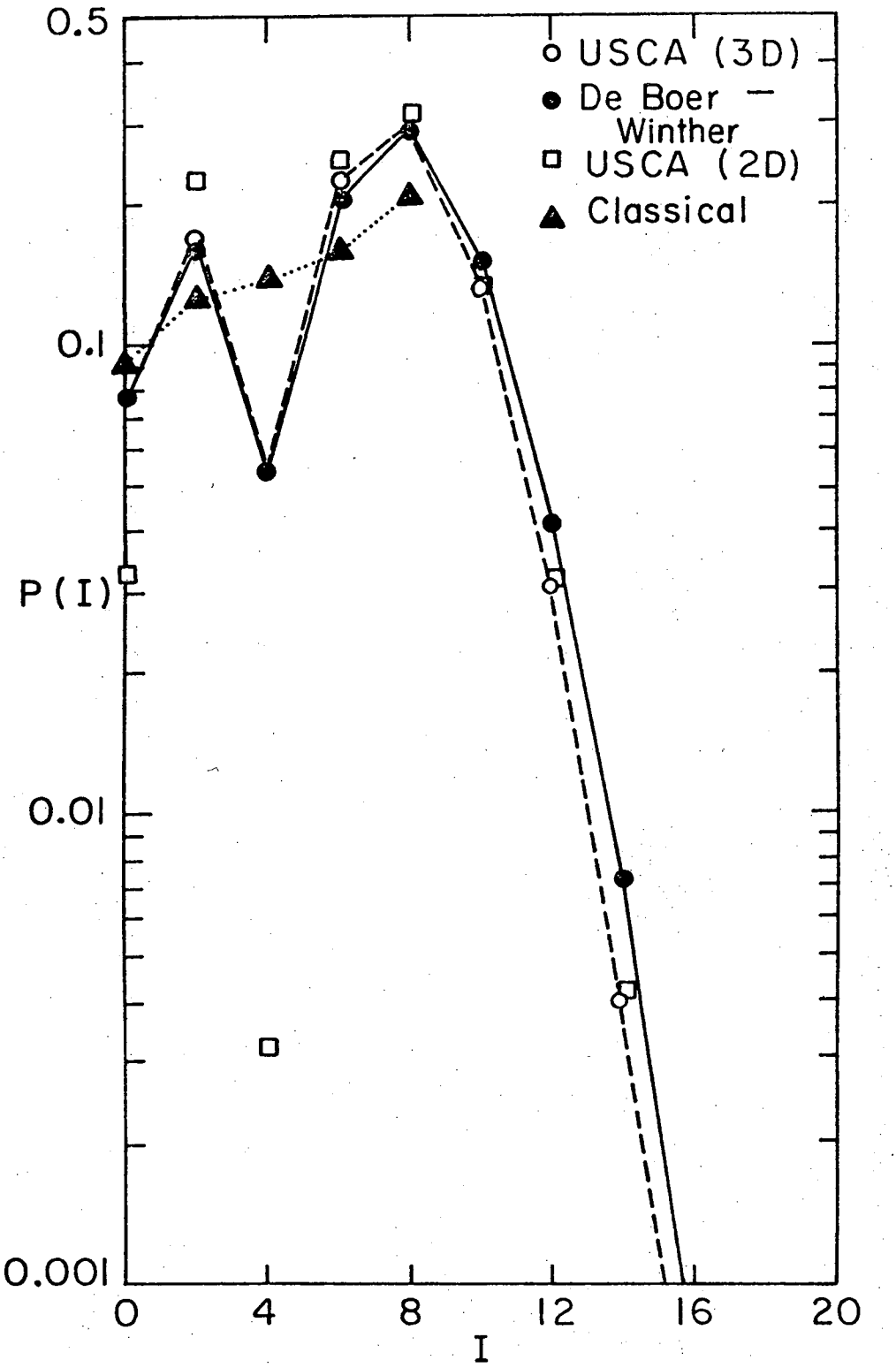
0.5
0.1
0.01
0.001
P(I)
0
4
8
12
16
20
I
USCA (3D)
De Boer — Winther
USCA (2D)
Classical
XBL7410-4542

Fig. 6

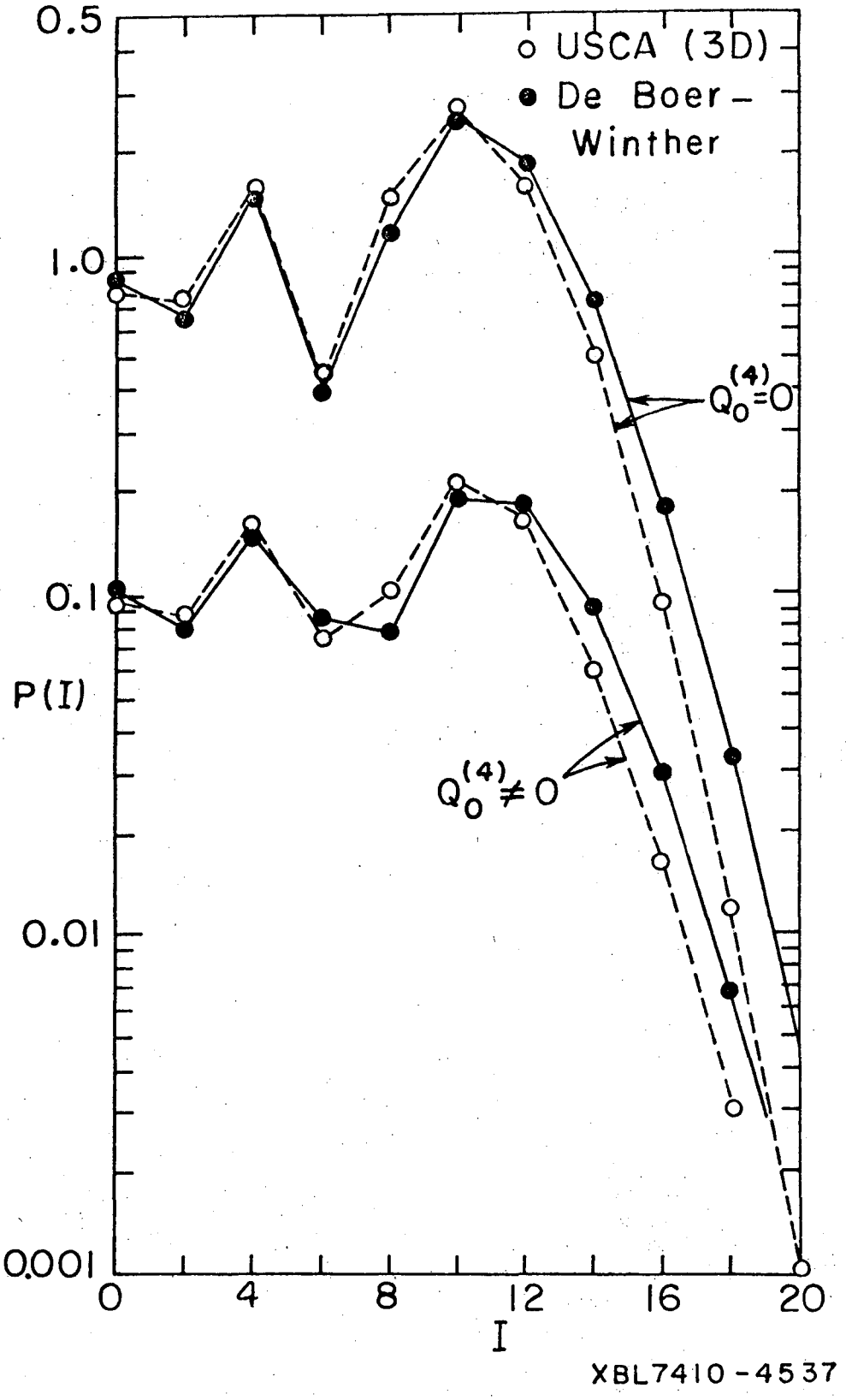
0.5
1.0
0.1
0.01
0.001
P(I)
0
4
8
12
16
20
I
USCA (3D)
De Boer-
Winther
$Q_0^{(4)}=0$
$Q_0^{(4)}\neq 0$
XBL7410-4537

Fig. 7

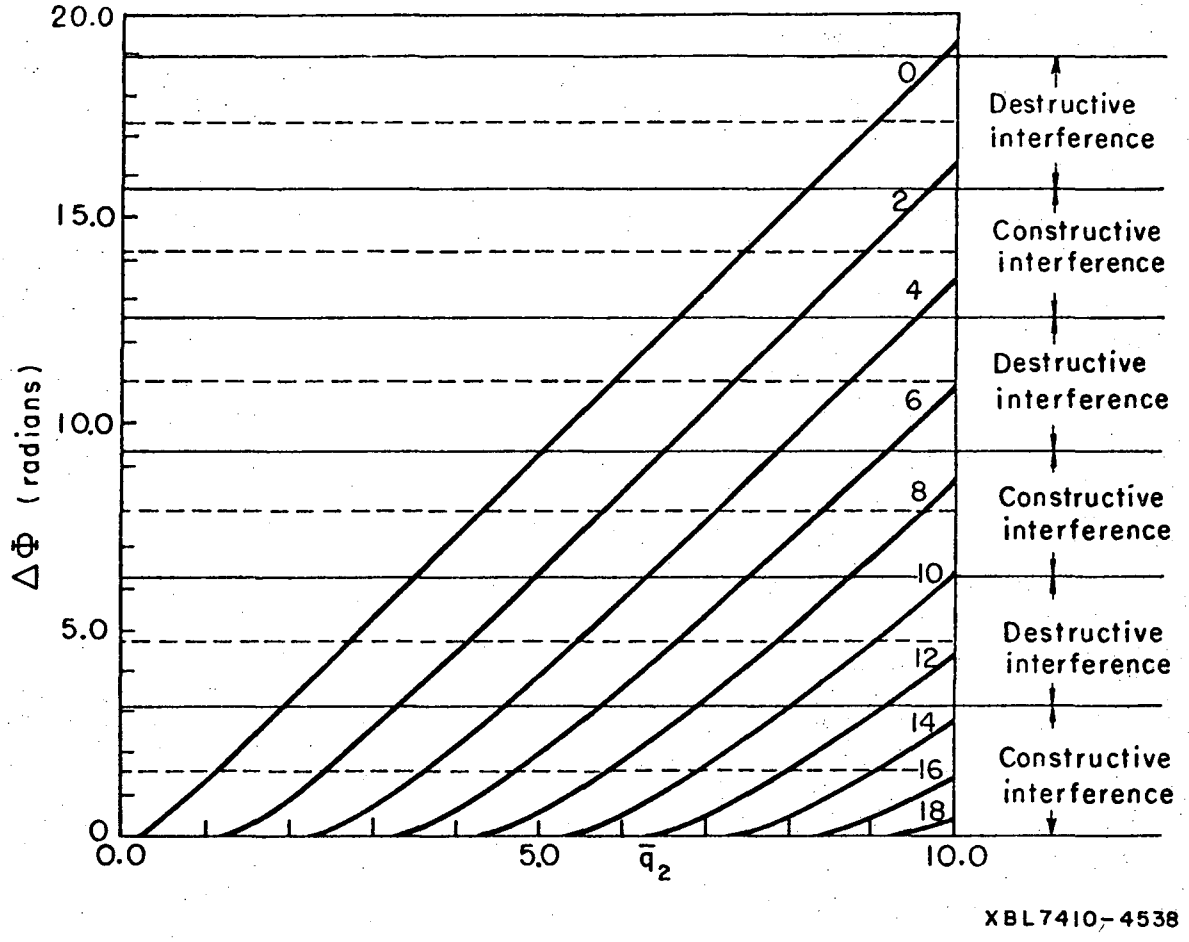
20.0
15.0
10.0
5.0
0
ΔΦ (radians)
0.0
5.0
$\bar{q}_2$
10.0
0
2
4
6
8
10
12
14
16
18
Destructive interference
Constructive interference
Destructive interference
Constructive interference
Destructive interference
Constructive interference
XBL7410-4538

Fig. 8

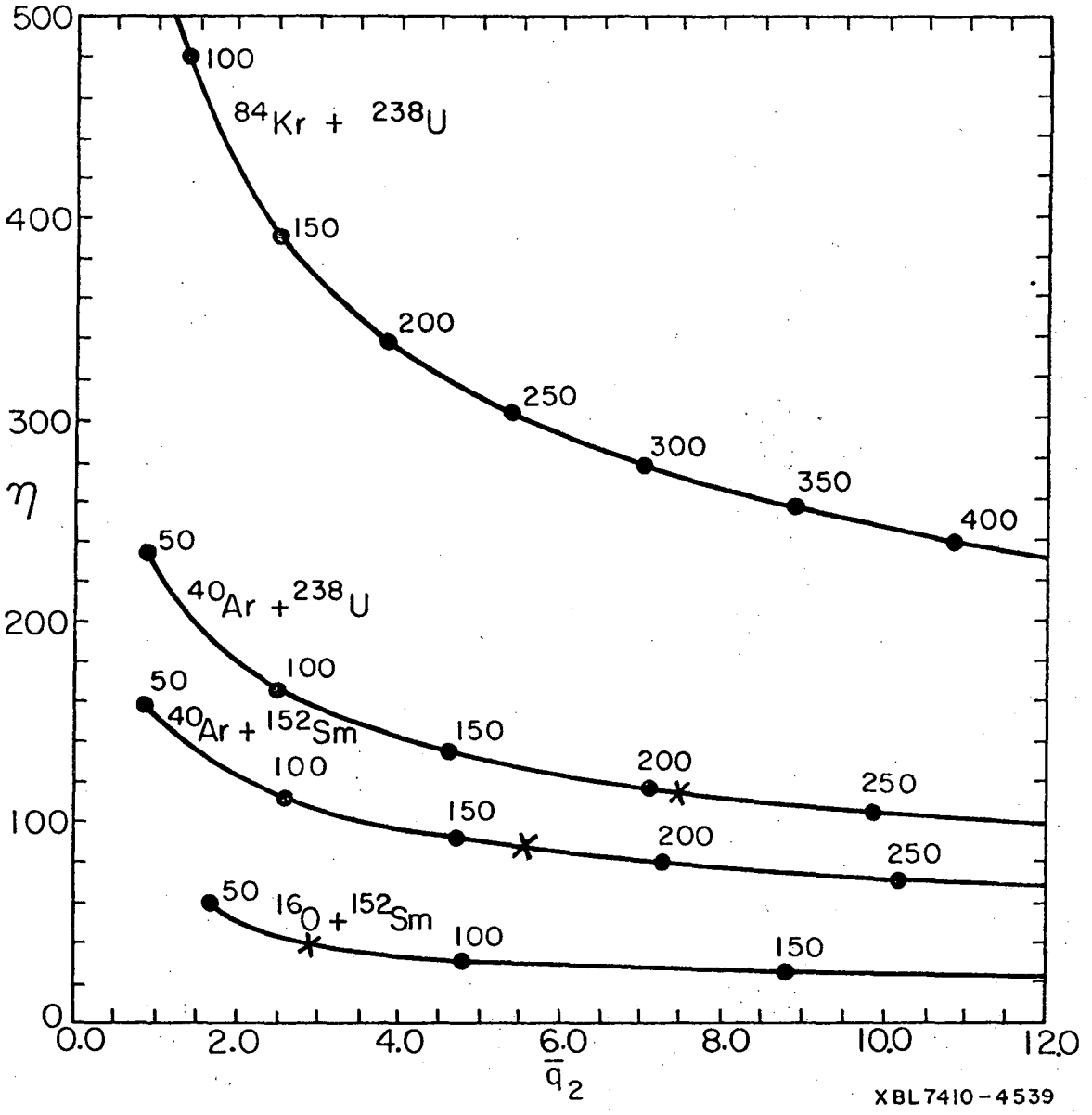
500
400
300
200
100
0
η
100
84Kr + 238U
150
200
250
300
350
400
50
40Ar + 238U
100
150
200
250
50
40Ar + 152Sm
100
150
200
250
50
16O + 152Sm
100
150
0.0
2.0
4.0
6.0
8.0
10.0
12.0
q̄2
XBL7410-4539

Fig. 9

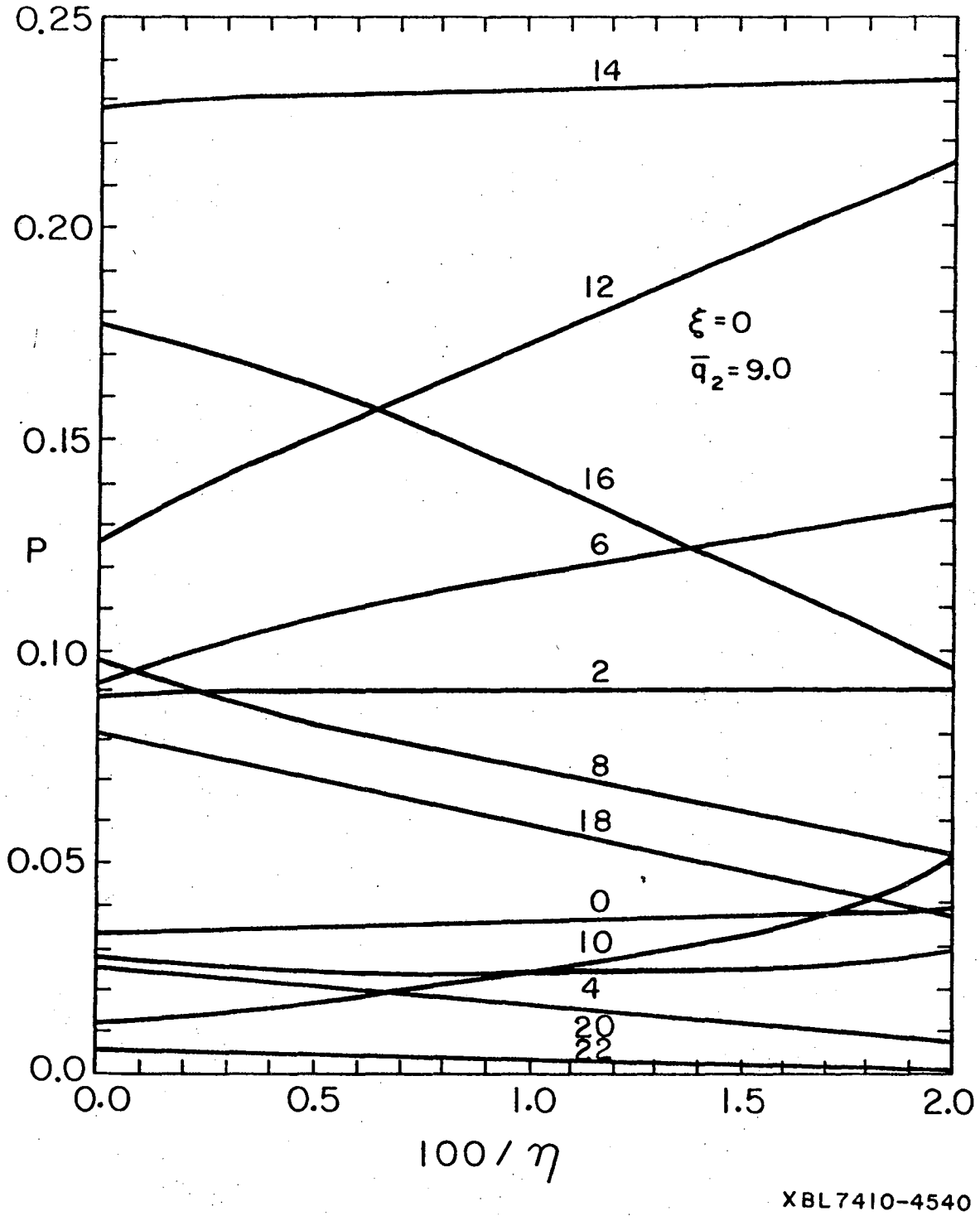
0.25
0.20
0.15
0.10
0.05
0.0
P
0.0
0.5
1.0
1.5
2.0
100 / η
14
12
16
6
2
8
18
0
10
4
20
22
ξ = 0
q̄₂ = 9.0
XBL7410-4540

Fig. 10

TECHNICAL INFORMATION DIVISION
LAWRENCE BERKELEY LABORATORY
UNIVERSITY OF CALIFORNIA
BERKELEY, CALIFORNIA 94720